Demonstration of the Applicability of 2-Look Burst Modes in Non-Stationary Scenarios with TerraSAR-X

Pau Prats-Iraola, German Aerospace Center (DLR), Pau.Prats@dlr.de, Germany
Nestor Yague-Martinez, German Aerospace Center (DLR), Nestor.Yague@dlr.de, Germany
Steffen Wollstadt, German Aerospace Center (DLR), Steffen.Wollstadt@dlr.de, Germany
Thomas Kraus, German Aerospace Center (DLR), Thomas.Kraus@dlr.de, Germany
Rolf Scheiber, German Aerospace Center (DLR), Rolf.Scheiber@dlr.de, Germany

Abstract

Burst-mode interferograms result in phase jumps between bursts in the presence of azimuthal motion. Such jumps occur due to the sudden change in the line-of-sight (LOS) vector (or, equivalently, the Doppler centroid) between consecutive bursts as a consequence of the burst mode operation. While the phase jumps might look like a nuisance, they are indeed the result of a legitimate measurement, namely, the azimuthal motion projected into the LOS vector. The phase jumps might complicate the phase unwrapping process and the exploitation and interpretation of the differential phase. While it is not always possible to handle the phase jumps with 1-look data, the use of 2-look acquisitions can considerably help in the proper decoupling of the range and azimuthal components of the motion. This paper presents the rationale to exploit 2-look data for that purpose. Data acquired with TerraSAR-X over the Petermann glacier in 2-look TOPS and ScanSAR modes are used to demonstrate the applicability of the approach, which is very useful in non-stationary scenes like glaciers or earthquakes.

1 Introduction

Burst modes allow the increase of the swath coverage at the expense of azimuthal resolution. However, the burst-mode operation has also an impact on the requirements in terms of interferometric performance. As shown in [1, 2], burst modes require of a higher coregistration accuracy in the azimuthal dimension in order to avoid phase jumps between bursts. The high-demanding coregistration requirements, in the order of 1-3 cm for TerraSAR-X, result from the linear variation of the Doppler centroid within a burst. In the TOPS case, the Doppler centroid variation is accentuated by the steering of the antenna from backward to forward, resulting in Doppler centroids in the order of a factor 3 larger than in the ScanSAR case.

If the coregistration is not performed with the required accuracy, the interferogram will present phase jumps at burst and sub-swath edges. In general, the accuracy can be achieved for stationary scenes, i.e., scenes where no significant azimuthal motion is present, by exploiting the spectral separation at the overlap area between bursts [1, 2]. However, burst-mode interferograms of scenes experiencing large azimuthal displacements, e.g., glaciers or earthquakes, will show evident phase jumps between bursts. The phase jumps are not an artifact but rather an indication of a true displacement, as the measured displacement is the result of projecting the motion vector into the line-of-sight, which is non-orthogonal to the along-track dimension at burst edges [3]. If phase jumps are to be removed, e.g., in order to ease the phase unwrapping, it is necessary to decouple the along-track motion of the scene from the across-track one. While some approaches can achieve a satisfactory performance by estimating the azimuthal motion using cross-correlation techniques [4], in practice one is limited by the performance of those approaches, which cannot measure the motion at the same spatial resolution as that of the interferometric phase. On the other hand, the overlap area is limited to a small extend of less than 10% of the azimuth burst length, hence resulting insufficient.

Two-look burst modes offer the opportunity to circumvent the aforementioned limitation occurring in conventional 1-look burst modes. This is done by exploiting the spectral separation between the two looks. Thanks to the 2-look operation, the large spectral separation is achieved for the complete swath without gaps. The present contribution analyses the potential of 2-look burst modes to decouple the across- and along-track displacements and proposes a rationale to process the data for non-stationary scenarios. The proposed approach is validated with TerraSAR-X data acquired over the Petermann glacier using the experimental 2-look ScanSAR and 2-look TOPS modes.

Section 2 revisits the coregistration requirement in burst modes, while Section 3 presents the rationale to exploit the 2-look burst mode for the decoupling of the along-track and across-track motions. Section 4 evaluates the performance in the estimation of the along-track shift for the proposed modes. Finally, Section 5 presents two examples with TerraSAR-X 2-look data.

2 Coregistration Requirements in Burst Modes

As described in [1, 2], in the presence of an azimuth coregistration error and a non-zero Doppler centroid, the interferometric phase has an additional component that adds to the zero-Doppler phase, given by

$$\varphi_{\text{az}} = 2\pi \cdot f_{\text{dc}}(r, x) \cdot \Delta t(r, x), \tag{1}$$

where r and x are the slant-range and azimuth coordinates, respectively, $f_{\text{dc}}(r, x)$ is the Doppler centroid and $\Delta t(r, x)$ is the azimuth coregistration error (in seconds). In burst modes, the Doppler centroid varies linearly along azimuth and mildly in range, so that a constant azimuth offset for the complete burst results in an azimuth phase ramp, as discussed in [2]. In the presence of heterogeneous azimuth coregistration errors, as could be the case in non-stationary scenarios, the interferometric phase will be as described by (1). As shown in [3], eq. (1) is indeed the phase contribution due to the projection of the azimuthal motion into the LOS. Ergo, φ_{az} should not be considered as a phase bias, but as a legitimate measurement of the azimuthal motion.

The bottom images of Figures 4 and 6 show the original phase of a 2-look ScanSAR and 2-look TOPS interferogram over the Petermann glacier, respectively. Phase jumps can be observed on over the moving parts of the glacier, especially in the TOPS interferogram, where the Doppler centroid variations are larger than in ScanSAR. The GIMP DEM [5] was used to remove the topographic component.

As suggested in [4], one option to remove the component in the DInSAR phase due to the azimuthal motion is by estimating first the azimuthal motion using an advanced filtering approach by exploiting in cascade cross-correlation and spectral diversity techniques along the azimuth dimension. However, due to the large averaging windows required in order to achieve the required accuracy not to bias the DInSAR phase, the approach cannot estimate the motion locally. In other words, the major assumption of the technique is that the motion gradient is highly correlated in space. If this condition is not met, the results after the correction might still show phase jumps. The following section shows the rationale to achieve a proper decoupling of the range and azimuth components of the motion by exploiting 2-look burst-mode data.

3 2-Look Burst Modes

The simple idea of 2-look data is to observe the same target on ground two times within a data take. In burst modes this can be achieved at the expense of either azimuth resolution or coverage. In the results presented in Section 5, the former has been selected.

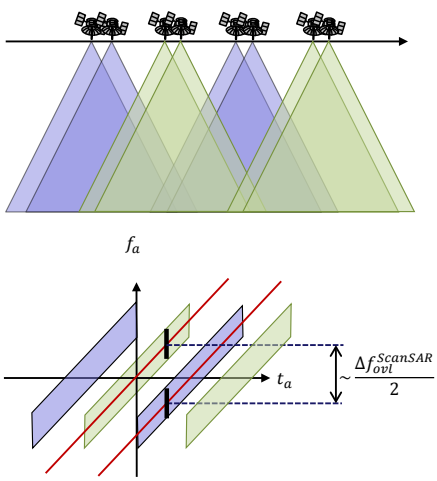

Figure 1: (Top) Sketch of a 2-look ScanSAR data take for one given sub-swath. (Bottom) Time frequency diagram of four bursts, where the two different colors indicate the two different looks.

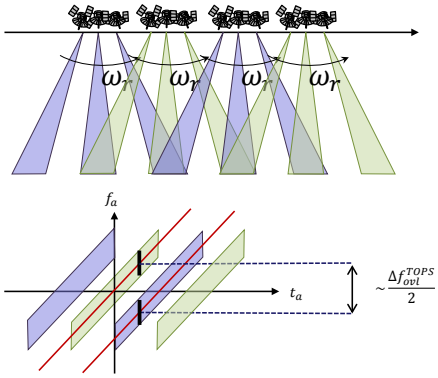

Figure 2: (Top) Sketch of a 2-look TOPS data take for one given sub-swath. (Bottom) Time frequency diagram of four bursts, where the two different colors indicate the two different looks.

Figures 1 and 2 show the rationale of the 2-look for ScanSAR and TOPS, respectively. The spectral separation for a target on ground between two consecutive bursts (looks) can be exploited in interferometry to retrieve an accurate estimation of the azimuthal motion. From an interferometric pair, two 1-look interferograms can be generated, which when combined, result in a differential interferogram, whose phase is given by

$$\varphi_{\text{SD}} = 2\pi \cdot \Delta f_{\text{ovl}}(r, x) \cdot \Delta t(r, x) \tag{2}$$

where Δf_{ovl} is now the spectral separation between the looks. The subscript SD stands for spectral diversity to follow the same nomenclature as in [1]. Since Δf_{ovl} is very large, the exploitation of the two looks allows the retrieval of $\Delta t(r, x)$ with very good accuracy and spatial resolution. It can be shown that the phase noise of the correction as given by (1) is given by [2]

$$\sigma_{\varphi_{\text{az}}} = \frac{2\sigma_{\text{int}}}{\sqrt{2}}, \tag{3}$$

where $\sigma_{\rm int}$ is the phase noise of the interferometric phase. Therefore, strictly speaking, it is sufficient to average 2 independent samples to have an estimate with the same noise level as the interferometric phase. In practice, some more samples can be averaged, especially in the range dimension, where the resolution is usually better in burst modes. A further aspect to consider is that $\varphi_{\rm SD}$ might be wrapped if the motion gradient is large. Note that the unambiguous range of the azimuth shifts is given by $\pm 1/(2\Delta f_{\rm ovl})$. Therefore, one option might be to unwrap the spectral diversity phase, a procedure that is in any case mandatory in conventional DInSAR techniques.
By using (2) it is possible to retrieve an accurate estimate of $\Delta t(r,x)$, which is then used to remove the azimuthal component of the motion from the differential phase (for both looks). This can be done by resampling the slave image using that information, or by correcting only the phase using (1). Finally, the final interferogram results free of jumps, where one can obviously add coherently the two corrected looks for noise reduction.

4 Azimuth Shift Estimation Performance

Figure 3 shows the predicted performance in the estimation of the azimuth shifts for the different modes by slightly modifying the equations provided in [6] in order to consider different bandwidths and spectral separations. The plot was generated assuming an input patch size of 100 m, which will result in different effective number of looks depending on the azimuth bandwidth. Table 1 shows the look bandwidth, the spectral separation and the azimuth resolution for the different modes under consideration. For comparison with the 2-look modes, the table includes also the stripmap mode, the BiDiSAR mode [7] (see [8]) and squinted acquisitions with $\pm 1^\circ$ squint. From Fig. 3 one can observe that the performance of the 2-look TOPS mode is close to the stripmap one, even if there is a factor 13 between the azimuth resolutions (3 m vs 38 m). For ScanSAR the performance is much worse since in this case the Doppler span within a burst is smaller than in TOPS. On the other hand, it is clear that BiDi outperforms the other modes owing to the large spectral separation, followed closely by the squinted stripmaps with $\pm 1^\circ$ squint.
It can be shown that the performance ratio between two given modes in the estimation of the azimuth shift is given by [8]

$$\rho = 10 \cdot \log_{10} \frac{\Delta f_1^2 \cdot B_{look,1}}{\Delta f_2^2 \cdot B_{look,2}}, \qquad (4)$$

where Δf_i is the spectral separation and $B_{look,i}$ is the azimuth bandwidth of one look, which for all modes is equal to B but for stripmap, where it is equal to $B/3$ [6]. For the given examples, the gains w.r.t. the stripmap mode are 29.8 dB, 24.4 dB, -1.38 dB and -11.01 dB, for BiDi, squinted SMs, 2-look TOPS and 2-look ScanSAR, respectively. While BiDi offers the best performance, the 2-look options have a larger coverage (100 km vs 30 km for TerraSAR-X). TOPS outperforms ScanSAR thanks to the antenna steering, which allows a larger Doppler centroid variation within the burst, and hence, a larger sensitivity to the along-track motion.

Table 1: Parameters for the performance evaluation

Mode	B	Δf	δx
Stripmap	2765 Hz	1843 Hz	3.0 m
BidiSAR	2000 Hz	38900 Hz	4.1 m
Squinted SMs	2765 Hz	17685 Hz	3.0 m
2-look TOPS	214 Hz	3200 Hz	38.7 m
2-look ScanSAR	205 Hz	1100 Hz	40.4 m

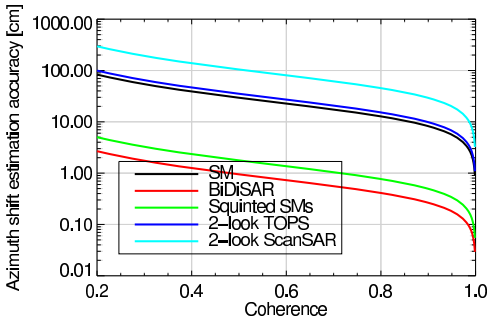

Figure 3: Accuracy in the estimation of the azimuth shift for different modes (see Table 1). An input patch size of 100 m has been assumed.

5 Results with TerraSAR-X

In order to demonstrate the potential of 2-look modes, experimental TerraSAR-X data takes have been commanded over the Petermann glacier, which already represents a challenging scenario due to the heterogeneous motion gradient present. Two pairs of ScanSAR and TOPS images have been acquired with a repeat-pass of eleven days. The ScanSAR data takes are composed of three sub-swaths and 549 bursts (with each burst being approx. 3 km long) and the TOPS data takes have four sub-swaths and 122 bursts (with a length of approx. 10 km each). The range coverages are 130 km and 100 km, respectively, with a total scene length of 500 km.
Figure 4 shows the original ScanSAR differential interferogram (after removing the DEM [5]), where the phase jumps between bursts can be hardly appreciated due to the small Doppler differences between contiguous bursts of about 1.1kHz. Figure 5(top) shows the phase of the differential interferogram between the two looks, i.e., the spectral diversity phase, which clearly shows the azimuthal motion of the glacier. In this interferogram one fringe represents about 6m, since the look separation is about 1.1kHz. Besides the motion of the glacier, also jumps between bursts can be observed. They mainly occur due to due the small differences in the spectral separation between looks, which depends on the scanning

pattern of the timeline. By properly unwrapping and scaling the SD phase using (2), the interferogram in Figure 4(bottom) can be corrected in order to obtain the final interferogram shown in Figure 5, which is now free of jumps. Note that in this interferogram the motion corresponds exactly to the across-track direction, since we have been able to remove the along-track component by exploiting the two looks.

Figure 6 shows now the results with TOPS. In the original differential interferogram the phase jumps between bursts are much clear than in the ScanSAR case, as the Doppler variation within a burst is larger due to the antenna steering. Figure 7(top) shows the phase of the differential interferogram between the two looks, i.e., the spectral diversity phase, which clearly shows the azimuthal motion of the glacier. In this interferogram, since the look separation is about 3200Hz one fringe represents about 2.2m. Besides the motion of the glacier, also jumps between bursts can be observed, similar as in the ScanSAR case. However, the main reason in the TOPS case are ionospheric disturbances that move between the acquisition of the bursts, hence introducing different azimuth shifts for contiguous bursts. After unwrapping and scaling the SD phase, the interferogram in Figure 6(bottom) can be corrected in order to obtain the final interferogram shown in Figure 7, which is now free of jumps.

6 Summary

This contribution has presented the exploitation of 2-look burst-mode data to decouple the azimuthal and range displacements from the differential phase. Such decoupling is necessary in non-stationary scenarios with large motion gradients. The coupling by itself is not a problem, but the Doppler centroid variation in burst modes together with azimuth coregistration errors (due to the motion) introduces phase offsets, which can result in phase jumps at burst edges, hence complicating the phase unwrapping and interpretation of the differential phase.

The rationale has been briefly presented and exemplary results have been shown with experimental TerraSAR-X ScanSAR and TOPS data acquired in the 2-look mode.

References

[1] R. Scheiber and A. Moreira. Coregistration of interferometric SAR images using spectral diversity. *IEEE Trans. Geosci. Remote Sens.*, 38(5):2179–2191, July 2000.

[2] P. Prats, R. Scheiber, L. Marotti, S. Wollstadt, and A. Reigber. TOPS interferometry with TerraSAR-X. *IEEE Trans. Geosci. Remote Sens.*, 50(8):3179–3188, August 2012.

[3] F. De Zan, P. Prats-Iraola, R. Scheiber, and A. Rucci. Interferometry with TOPS: coregistration and azimuth shifts. In *Proceedings of EUSAR*, 2014.

[4] R. Scheiber, M. Jaeger, P. Prats-Iraola, F. De Zan, and D. Geudtner. Speckle tracking and interferometric processing of TerraSAR-X TOPS data for mapping nonstationary scenarios. *IEEE JSTARS*, 8(4):1709–1720, April 2015.

[5] I.M. Howat, A. Negrete, and B.E. Smith. The Greenland ice mapping project (GIMP) land classification and surface elevation data sets. *The Cryosphere*, 8(4):1509–1518, 2014.

[6] R. Bamler and M. Eineder. Accuracy of differential shift estimation by correlation and split-bandwidth interferometry for wideband and Delta-k SAR systems. *IEEE Geosci. Remote Sens. Lett.*, 2(2):151–155, April 2005.

[7] Josef Mittermayer, Steffen Wollstadt, Pau Prats-Iraola, Paco López-Dekker, Gerhard Krieger, and Alberto Moreira. Bidirectional SAR imaging mode. *IEEE Trans. Geosci. Remote Sens.*, 51(1):601–614, January 2013.

[8] P. Prats-Iraola, M. Rodriguez-Cassola, N. Yague-Martinez, P. Lopez-Dekker, R. Scheiber, F. De Zan, T. Kraus, and S. Wollstadt. Repeat-pass interferometric experiments with the TanDEM-X constellation for accurate along-track motion estimation. In *Proceedings of IGARSS*, 2015.

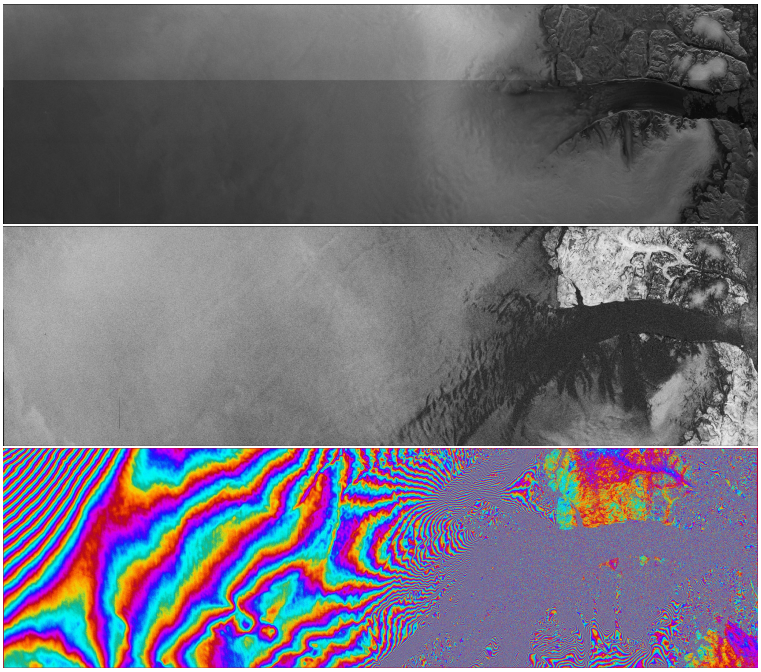

Figure 4: ScanSAR interferogram over the Petermann glacier, Greenland. (Top) Reflectivity image. (Middle) Interferometric coherence. (Bottom) Original differential interferogram, where the jumps between bursts, while small, can still be appreciated (see zooms of Figure 5.

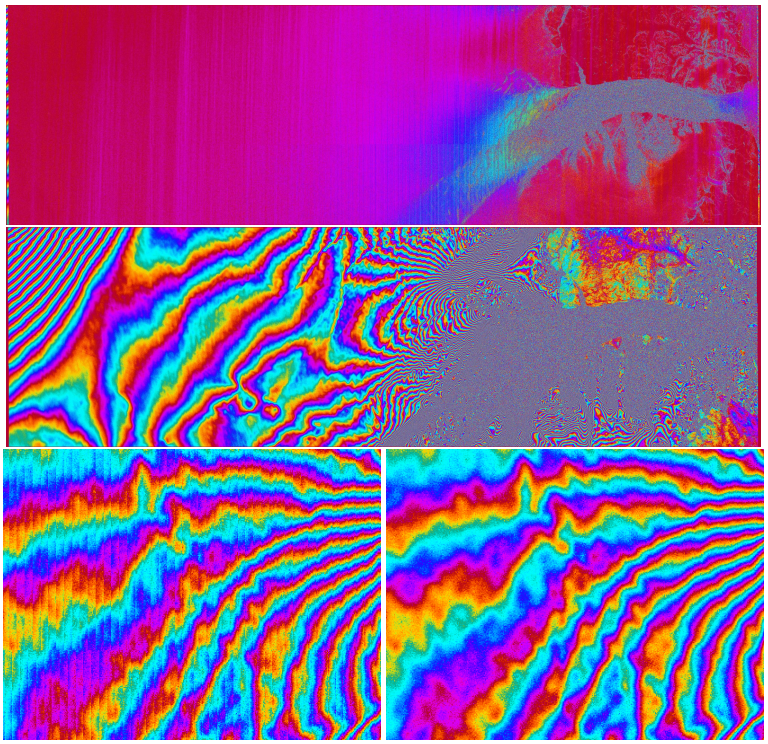

Figure 5: ScanSAR interferogram over the Petermann glacier, Greenland. (Top) Differential interferogram between the two looks, where the along-track motion can be clearly observed. (Middle) Corrected differential interferogram after removing the azimuthal component of the motion by exploiting the 2-looks (see Figure 4). (Bottom) Zoom of the original and corrected phases.

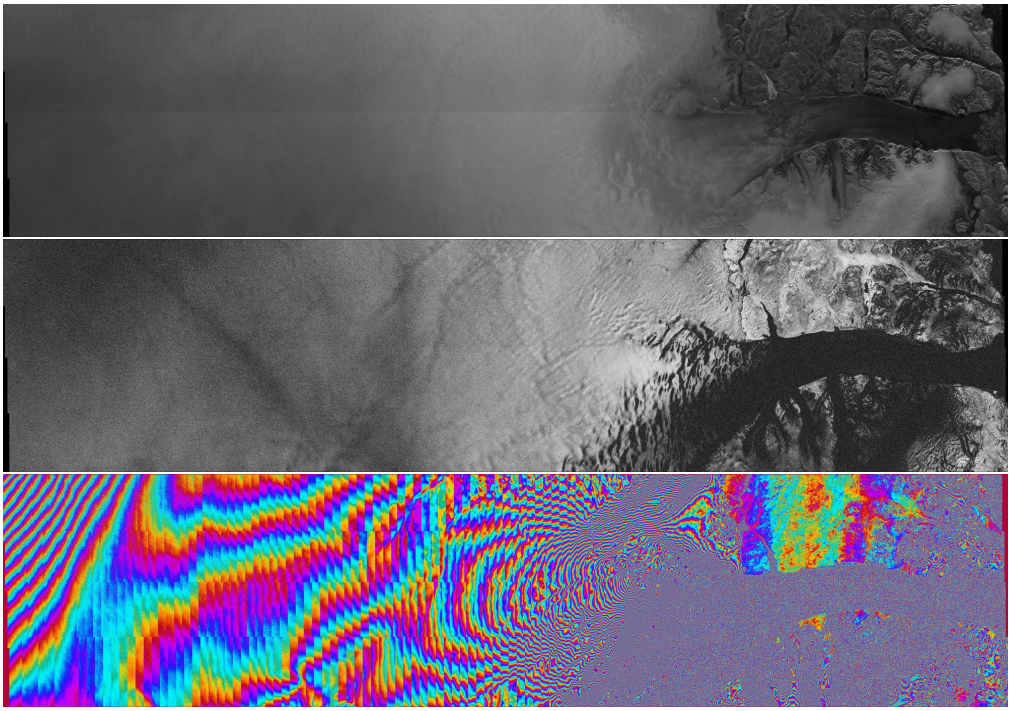

Figure 6: TOPS interferogram over the Petermann glacier, Greenland. (Top) Reflectivity image. (Middle) Interferometric coherence. (Bottom) Original differential interferogram.

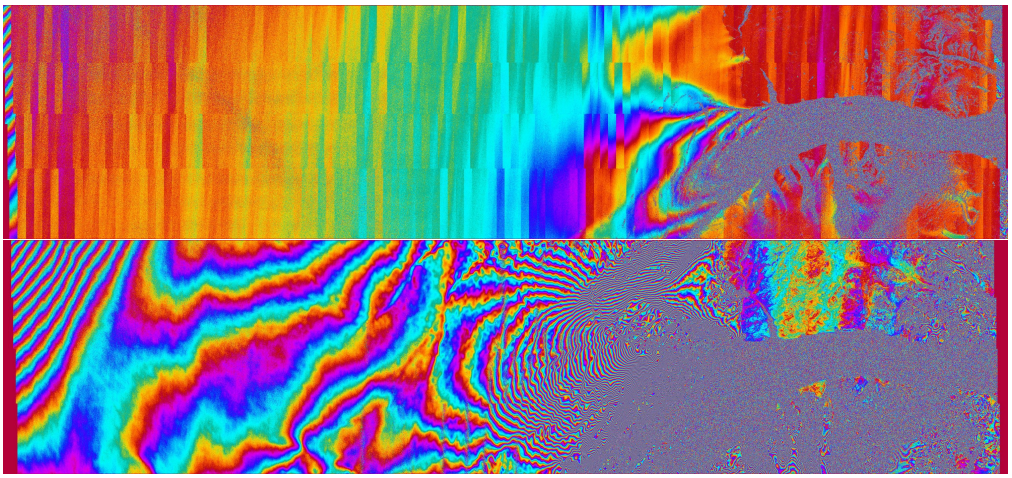

Figure 7: TOPS interferogram over the Petermann glacier, Greenland. (Top) Differential interferogram between the two looks, where the along-track motion can be clearly observed. The jumps between bursts are mainly attributed to ionospheric disturbances. (Bottom) Corrected differential interferogram after removing the azimuthal component of the motion by exploiting the 2-looks (see Figure 6).